Dalton Transactions

An international journal of inorganic chemistry

Accepted Manuscript

This article can be cited before page numbers have been issued, to do this please use: N. Busto, M. C. Carrión, S. Montanaro, B. Diaz de Greñu, T. Biver, F. A. Jalon, B. R. Manzano and B. Garcia, *Dalton Trans.*, 2020, DOI: 10.1039/D0DT02125C.

ROYAL SOCIETY OF CHEMISTRY

rsc.li/dalton

View Article Online
DOI: 10.1039/D0DT02125C

Targeting G-Quadruplex structures with Zn(II) terpyridine derivatives: a SAR study

Natalia Busto[a*], M. Carmen Carrión[b], Sonia Montanaro [c], Borja Diaz de Greñu,[b] Tarita Biver [c, d], Felix A. Jalón[b*], Blanca R. Manzano[b*] and Begoña García [a*].

[a]Chemistry Department, University of Burgos, Pza. Misael Bañuelos s/n, 09001 Burgos, Spain (nataliabyv@msn.com; begar@ubu.es)

[b] Departamento de Química Inorgánica, Orgánica y Bioquímica, Facultad de Químicas (IRICA), Universidad de Castilla La Mancha, Avenida Camilo J. Cela 10, 13071 Ciudad Real, Spain (blanca.manzano@uclm.es; felix.jalon@uclm.es)

[c] Department of Chemistry and Industrial Chemistry, University of Pisa, Via Moruzzi, 13, 56124 Pisa, Italy

[d] Department of Pharmacy, University of Pisa, Via Bonanno Pisano 6, 56126 Pisa, Italy

KEYWORDS: Terpyridine, Zn(II) complexes, G-quadruplex, DNA binding, Cytotoxicity

ABSTRACT

Based on the ability of terpyridines to react with G-quadruplex DNA (G4) structures along with the interest aroused by Zn as an essential metal centre in many biological processes, we have synthesized and characterized six Zn chloride or nitrate complexes containing terpyridine ligands with different 4´-substituents. In addition, we have studied their interaction with G4 and their cytotoxicity.

Our experimental results revealed that the leaving group exerts strong influence in the cytotoxicity, since the complexes bearing chloride were more cytotoxic that their nitrate analogues and an effect of the terpyridine ligand was also observed. The thermal stabilization profiles showed that the greatest stabilization of hybrid G4, Tel22, was observed for the Zn complexes bearing the terpyridine ligand that contained one or two methylated 4-(Imidazol-1-yl)phenyl substituent, **3Cl** and **3(L)$_2$,** respectively, probably due to their extra positive charge. Stability and aquation studies for these complexes were carried out and no release of ligand was detected. Complexes **3Cl** and **3(L)$_2$** were successfully internalized by SW480 cells and they seemed to be localized mainly in the nucleolus. Highest cytotoxicity, G4 selectivity, G4 affinity, determined by fluorescence and ITC experiments, and subcellular localization, quantified by ICP-MS measurements, rendered **3Cl** a very interesting complex from a biological standpoint.

View Article Online
DOI: 10.1039/D0DT02125C

INTRODUCTION

Guanine rich nucleic acid sequences able to form G-quadruplexes DNA (G4) structures play key cellular regulatory roles and are considered as promising targets for anticancer therapy. Here, G-tetrads are planar squares formed by four guanines interacting by Hoogsten hydrogen bonds.[1] The self-stacking of two or more G-tetrads further stabilized by the presence of a monovalent cation in the central channel leads to the formation of G4. These non-canonical nucleic acids secondary structures are highly polymorphic enabling the design of specific G4-ligands.[2,3] The identification of more than 700,000 potential quadruplex-forming sequences in the human genome[4] has contributed to immensely attract researchers' attention. As a consequence of this intense research on G4, evidences not only for their existence *in cellulo* but also for their involvement in a great number of biological processes such as telomere stability, replication, transcription and translation have been provided.[5–7] Indeed, G4s constitute an important focus of attention in drug development due to their potential as therapeutic agents for cancer, neurological and infectious diseases.[8–13]

In this scenery, the search for G4-binders able to selectively interact with G4s over duplex structures or even more, to selectively interact with a specific G4 topology, represents a key step for this research field.[14,15] Among them, metal complexes have emerged as promising alternatives to conventional organic compounds due to their relative easy synthesis and tunable properties by changing the metal center or the ligands.[16,17]

On the one hand, terpyridines (tpy) are well-known nitrogen tridentate ligands with great metal coordination ability that have been extensively applied in material and medicinal chemistry.[18–22] In fact, coordination complexes with the terpyridine ligand and its derivatives with several substituents in the 4' position have been widely investigated due to their potential applications in diverse fields as luminescence,[23] catalysis,[24] supramolecular chemistry,[18,19] in dye-sensitized solar cells,[24] and also in the biomedical domain.[25] More specifically, complexes with 4'-substituted-terpyridine and metals as Pt(II), Cu(II) and Pd(II) palladium have been extensively investigated due to their planar geometry which facilitate π-stacking interactions with the G-tetrad.[26–31] Bimetallic species have also been described by the group of R. Vilar.[32,33] In general, it is found a clear influence in the biological activity of the substituent in the terpyridine ligand and the metal centre.

On the other hand, Zn is the second most abundant essential trace element in the human body being an essential cofactor of more than 300 enzymes and 1000 transcription factors. That is, this essential metal plays a crucial role in a lot of biological processes ranging from growth, immune response and neurological processes.[34–37] Thus, the ability to interact with G-quadruplex structures of Zn derivatives with classic G4 binders scaffolds such as porphyrins or salphen-like ligands has been described.[38–40] Recently, the interaction of some Zn(II) benzoate terpyridine derivatives with ctDNA by intercalation and with G-quadruplexes by external binding has been described.[41] Even though, the field of Zn(II) terpyridines derivatives as G4-binders is quite unexplored respecting Pt(II) or Cu(II) derivatives. The importance of metal geometry in the recognition of G4-DNA by metal-terpyridine complexes has been previously studied.[42] It has been reported that the complex $[Zn(L)(NO_3)_2]$ (L = 4-([2,2':6',2''-terpyridin]-4'-yl)-N,Ndiethylaniline) inhibited telomerase by

View Article Online
DOI: 10.1039/D0DT02125C

interacting with c-myc G-quadruplex DNA and induced cell cycle arrest at the S phase.[43] Promising *in vitro* anti-tumour activities in tpy Zn derivatives have also been reported, both for $[Zn(R\text{-}tpy)X_2]$[44–47] and $[Zn(R\text{-}tpy)_2]X_2$ type[48] (X = anion) complexes.

Therefore, six Zn(II) complexes with terpyridine derivatives were synthesized and characterized in this work. The ligands used, 4′-functionalized 2,2′:6′,2″-terpyridines (4′R-tpy), are reflected in Figure 1. Their design has several objectives: i) the use of extended terpyridines which are more favourable to target quadruplex-DNA than tpy;[31,42] ii) the introduction of basic substituents in the planar π–π stacking core, that could give rise to the formation of hydrogen bonds and enhance their interactions with G4; iii) the addition, in the case of **L3,** of an extra positive charge to increase the electrostatic interaction with the negative charged DNA, as it has already observed for N-methylated quinacridines.[49] Two kind of anions and two different formulations with one or two coordinated ligands were explored. The global objective of all these modifications was to extract structure-activity relationships. Their cytotoxicity in human tumour cells and their ability to stabilize G4 structures were evaluated. In the light of these results, the most interesting Zn(II) terpyridine derivatives were further studied. Their cellular uptake and their ability to target G4 was explored by means of fluorescence microscopy, ICP-MS measurements, UV-vis, fluorescence, circular dichroism spectroscopies and Förster resonance energy transfer (FRET) melting assays.

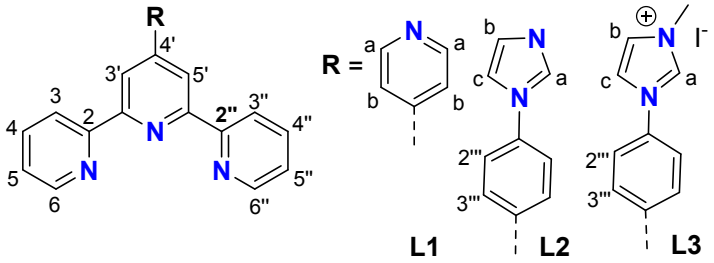

Figure 1. Ligands **L1**-**L3** used in this work and atom numbering scheme

EXPERIMENTAL SECTION

Reagents and solvents used were of commercially available reagent quality unless otherwise stated. Solvents were distilled from the appropriate drying agents and degassed before use. Elemental analyses were performed with a Thermo Quest FlashEA 1112 microanalyzer. Fast atom bombardment mass spectra (FAB MS) (position of the peaks in Da) were recorded with an Autospec spectrometer or a Thermo MAT95XP mass spectrometer with a magnetic sector. NMR spectra were recorded at 298 K on a Varian Unity Inova 400 or on a Varian Inova 500 spectrometer. ^{1}H NMR chemical shifts were internally referenced to tetramethylsilane (TMS) via the residual ^{1}H signals of CD_3OD. Chemical shift values are reported in ppm and coupling constants (J) in Hz. The splitting of proton resonances is defined as s = singlet, d = doublet, t = triplet, m = multiplet. COSY (COrrelation SpectroscopY) 2D NMR spectra were recorded using standard pulse–pulse sequences. All NMR data processing was carried out using MestReNova version 6.1.1. The solvent indicated in the elemental

View Article Online
DOI: 10.1039/D0DT02125C

analysis was detected in the corresponding ^{1}H NMR spectra. The synthesis and characterization of ligands **L1**-**L3**[50–52] is included in the Supporting Information (SI).

Synthesis and characterization of the complexes

1Cl. A suspension of 13.2 mg of $ZnCl_2$ (0.097 mmol) was prepared in 5 mL of dichloromethane (DCM). 30 mg of **L1** (0.097 mmol) were added over this suspension. 5 mL of CH_3CN were added and the suspension turned in colour to give a white precipitate. The reaction was stirred overnight. The resulting solid was filtrated, washed with DCM (5 mL) and dried under vacuum to give 36 mg (0.08 mmol, 83 % yield). M_r ($C_{20}H_{14}N_4Cl_2Zn$) = 446.64 g/mol. Anal. Calcd. for $H_{14}C_{20}N_4Cl_2Zn$: % C 53.78; H 3.16; N, 12.54. Found: C 53.45; H 3.04; N 12.14. ^{1}H-NMR: δ (CD_3OD, TMS) 9.10 (d, $H^{6,6''}$ tpy, J_{HH} = 4.3, 2H), 9.05 (s, $H^{3',5'}$ tpy, 2H), 8.85 (m, $H^{3,3''}$ tpy and $H^{a\ or\ b}$ py, 4H), 8.38 (t, $H^{4,4''}$ tpy, J_{HH} = 7.7, 2H), 8.14 (d, $H^{a\ or\ b}$ py, J_{HH} = 6.0, 2H), 7.91 (dd, $H^{5,5''}$ tpy, J_{HH} = 7.3, 4.6, 2H) ppm. MS (FAB+): m/z (%) = 409 (31) ([M-Cl]$^+$).

1NO$_3$. It was obtained in a similar way as that described for **1Cl** using $Zn(NO_3)_2.6H_2O$ (28.7 mg, 0.097 mmol) and 30 mg of **L1** (0.097 mmol). It was obtained as a white powder. Yield 37.8 mg (0.076 mmol, 78 %). M_r ($C_{20}H_{14}N_6O_6Zn$) = 499.74 g/mol. Anal. Calcd. for $C_{20}H_{14}N_6O_6Zn$: % C 48.07; H 2.82; N 16.82; Found: C 47.85; H 2.55; N 16.51. **1NO$_3$** appears in CD_3OD solution as a mixture of this complex and **1(L)$_2$** (**1NO$_3$**:**1(L)$_2$** ratio = 66:33) as consequence of the ligand coordination lability. ^{1}H-NMR δ (CD_3OD, TMS): 9.33 (s, $H^{3',5'}$ tpy,1(L)$_2$, 2H), 9.11 (s, $H^{3',5'}$ tpy, **1NO$_3$**, 2H), 8.99 (d, $H^{6,6''}$ tpy, **1NO$_3$**, J_{HH} = 4.8, 2H), 8.94 (m, $H^{b\ or\ c}$ py, **1NO$_3$**, $H^{3,3''}$ tpy, **1(L)$_2$**, $H^{a\ or\ b}$ py, **1(L)$_2$**, 6H), 8.86 (d, $H^{3,3''}$ tpy, **1NO$_3$**, J_{HH} = 5.3, 2H), 8.45 (t, $H^{4,4''}$ tpy, **1NO$_3$**, J_{HH} = 7.2, 2H), 8.28 (d, $H^{a\ or\ b}$ py, **1(L)$_2$**, J_{HH} = 6.2, 2H), 8.26 (t, $H^{4,4''}$ tpy, **1(L)$_2$**, J_{HH} = 7.7, 2H), 8.14 (d, $H^{a\ or\ b}$ py, **1NO$_3$**, J_{HH} = 6.1, 2H), 7.97 (m, $H^{5,5''}$ tpy, **1NO$_3$**, $H^{6,6''}$ tpy,**1 (L)$_2$**, 4H), 7.50 (t, $H^{5,5''}$ tpy, **1(L)$_2$**, J_{HH} = 6.0, 2H) ppm. MS (FAB+): m/z (%) = 436 (36) ([M-NO$_3$]$^+$).

2Cl. Complex **2Cl** was previously described[53] but the NMR data were not reported. It was obtained in a similar way as that described for **1Cl** using 14.5 mg of $ZnCl_2$ (0.11 mmol) and 40 mg of **L2** (0.11 mmol) to give 40.5 mg of complex **2Cl** (0.079 mmol, 72 % yield). Mr ($C_{24}H_{17}Cl_2N_5Zn$) = 511.71 g/mol. Anal. Calcd. for $C_{24}H_{17}Cl_2N_5Zn$: % C 56.33; H 3.35; N 13.69; Found: C 56.01; H 3.24; N 13.35. ^{1}H-NMR δ (CD_3OD, TMS): 9.08 (d, $H^{6,6''}$ tpy, J_{HH} = 4.6, 2H), 9.01 (s, $H^{3',5'}$ tpy, 2H), 8.85 (d, $H^{3,3''}$ tpy, J_{HH} = 8.0, 2H), 8.36 (td, $H^{4,4''}$ tpy, J_{HH} = 9.2, 1.3, 2H), 8.35 (s, H^a Im, 1H), 8.30 (d, $H^{2'''or3'''}$ Ph, J_{HH} = 8.7, 2H), 7.92 (d, $H^{2'''or3'''}$ Ph, J_{HH} = 8.8, 2H), 7.90 (dd, $H^{5,5''}$ tpy, J_{HH} = 7.1, 5.3, 2H), 7.76 (s, $H^{b\ or\ c}$ Im, 1H), 7.25 (s, $H^{b\ or\ c}$ Im, 1H) ppm. MS (FAB+): m/z (%) = 474 (100) ([M-Cl]$^+$).

2NO$_3$. It was obtained in a similar way as that described for **1Cl** using 23.8 mg of $Zn(NO_3)_2.6H_2O$ (0.08 mmol) and 30 mg of **L2** (0.08 mmol) to give 41.8 mg of complex **2NO$_3$** (0.066 mmol, 83 % yield). M_r ($C_{24}H_{17}N_7O_6Zn$) = 564.82 g/mol. Anal. Calcd for $C_{24}H_{17}N_7O_6Zn$: % C 51.04; H 3.03; N 17.36; Found: C 50.70; H 2.99; N 16.99. **2NO$_3$** appears in CD_3OD solution as a mixture of this complex and **2(L)$_2$** (**2NO$_3$**:**2(L)$_2$** ratio = 69:31) as consequence of the ligand coordination lability. ^{1}H-NMR δ (CD_3OD, TMS): 9.29 (s, $H^{3',5'}$ tpy, **2(L)$_2$**, 2H), 9.08 (s, $H^{3',5'}$ tpy, **2NO$_3$**, 2H), 8.95 (m, $H^{6,6''}$ tpy, **2NO$_3$**, $H^{3,3''}$ tpy, **2NO$_3$**, $H^{3,3''}$ tpy, **2(L)$_2$**, 6H), 8.47 (d, $H^{2'''or3'''}$ Ph, **2NO$_3$**, J_{HH} = 8.7, 2H), 8.44 (td, $H^{4,4''}$ tpy, **2NO$_3$**, J_{HH} = 7.8, 1.7, 2H), 8.43 (s, H^a Im, 1H), 8.38 (s, H^a Im, 1H), 8.32 (d, $H^{2'''or3'''}$ Ph, **2(L)$_2$**, J_{HH} = 8.8, 2H), 8.25 (td, $H^{4,4''}$

View Article Online
DOI: 10.1039/D0DT02125C

tpy, **2(L)$_2$**, J_{HH} = 7.9, 1.6, 2H), 8.02 (d, $H^{2'''or3'''}$ Ph, **2NO$_3$**, J_{HH} = 8.7, 2H), 7.96 (m, $H^{5,5''}$ tpy, **2NO$_3$**, $H^{6,6''}$ tpy, **2(L)$_2$**, $H^{2'''or3'''}$ Ph, **2(L)$_2$**, 6H), 7.83 (s, $H^{b\ or\ c}$ Im, 1H), 7.79 (s, $H^{b\ or\ c}$ Im, 1H), 7.50 (dd, $H^{5,5''}$ tpy, **2(L)$_2$**, J_{HH} = 7.5, 5.1, 2H), 7.29 (s, $H^{b\ or\ c}$ Im, 1H), 7.27 (s, $H^{b\ or\ c}$ Im, 1H) ppm. MS (FAB+): m/z (%) = 501 (28) ($[M\text{-}NO_3]^+$, 439 (7) ($[M\text{-}2NO_3]^+$).

3Cl. A suspension of 13.2 mg of $ZnCl_2$ (0.097 mmol) was prepared in 5 mL of DCM. 50 mg of **L3** (0.097 mmol) was added over this suspension. The suspension clarified as 5 mL of CH_3CN was added giving a pale-yellow solution. A white solid precipitated from this solution after stirring at room temperature overnight. The filtration of this precipitate and washing with 5 mL of DCM gave a pale-yellow solid that was dried under vacuum (53.9 mg, 85 %). M_r ($C_{25}H_{20}Cl_2N_5IZn$) = 653.65 g/mol. Anal. Calcd for $C_{25}H_{20}Cl_2N_5IZn.H_2O$: % C 44.71; H 3.30; N 10.43; Found: C 44.33; H 3.10; N 10.22. This solid is insoluble in DCM, soluble in DMSO and scarcely soluble in MeOH. ^{1}H-NMR δ (CD_3OD, TMS): 9.09 (d, $H^{6,6''}$ tpy, J_{HH} = 4.4, 2H), 9.04 (s, $H^{3',5'}$ tpy, 2H), 8.83 (d, $H^{3,3''}$ tpy, J_{HH} = 7.8, 2H), 8.43 (d, $H^{2'''or3'''}$ Ph, J_{HH} = 7.8, 2H), 8.36 (td, $H^{4,4''}$ tpy, J_{HH} = 6.9, 1.4, 2H), 8.25 (d, $H^{b\ or\ c}$ Im, J_{HH} = 2.0, 1H), 8.04 (d, $H^{2'''or3'''}$ Ph, J_{HH} = 7.8, 2H), 7.90 (dd, $H^{5,5''}$ tpy, J_{HH} = 6.9, 5.8, 2H), 7.88 (d, $H^{b\ or\ c}$ Im, J_{HH} = 2.0, 1H), 4.10 (s, MeIm, 3H) ppm. MS (FAB+): m/z (%) = 616 (26) ($[M\text{-}Cl]^+$), 581 (22) ($[M\text{-}2Cl]^+$), 526 (72) ($[M\text{-}I]^+$), 488 (100) ($[M\text{-}Cl\text{-}I\text{-}H]^+$).

3(L)$_2$. A suspension with 15.0 mg of $Zn(NO_3)_2{\cdot}6H_2O$ (0.050 mmol) was prepared in 5 mL of CH_2Cl_2. 52.2 mg of **L3** (0.101 mmol) were added over this suspension. The suspension clarified when 5 mL of CH_3CN were added giving a pale-yellow solution. A yellow solid precipitated from this solution after stirring at room temperature overnight. The filtration of this precipitate and washing with 5 mL of DCM gave a pale-yellow solid that was dried under vacuum (50 mg, 82 %). This solid is insoluble in DCM and soluble in MeOH and H_2O. Mr($C_{50}H_{40}I_2N_{12}O_6Zn$) = 1224,13 g/mol. % C 49.06; H 3.29; N 13.73; Found: C, 48.75; H 3.13; N, 13.57. ^{1}H-NMR (CD_3OD): δ(TMS): 9.32 (s, $H^{3',5'}$ tpy, 2H), 8.97 (d, $H^{3,3''}$ tpy, J_{HH} = 8.3, 2H), 8.60 (d, $H^{2'''or3'''}$ Ph, J_{HH} = 8.3, 2H), 8.29 (d, $H^{b\ or\ c}$ Im, J_{HH} = 1.9, 1H), 8.25 (t, $H^{4,4''}$ tpy, J_{HH} = 7.8, 2H), 8.12 (d, $H^{2'''or3'''}$ Ph, J_{HH} = 8.3, 2H), 8.00 (d, $H^{6,6''}$ tpy, J_{HH} = 4.4, 2H), 7.90 (d, $H^{b\ or\ c}$ Im, J_{HH} = 1.9, 1H), 7.51 (t, $H^{5,5''}$ tpy, J_{HH} = 6.8, 2H), 4.12 (s, MeIm, 3H). MS (FAB+): m/z (%) = 1160 (5) ($[M\text{-}NO_3]^+$), 1097 (10) ($[M\text{-}2NO_3\text{-}H]^+$), 1033 (28) ($[M\text{-}I\text{-}NO_3]^+$), 970 (30) ($[M\text{-}2NO_3\text{-}I\text{-}H]^+$), 844 (100) ($[M\text{-}2I\text{-}2NO_3]^+$), 390.

The dried human telomeric oligonucleotide Tel 22, d[AGGG(AGGGTT)$_3$], was purchased for Thermo Fisher Scientific Inc. The double-labelled oligonucleotides have as the donor fluorophore in the 5' end FAM (6-carboxyfluorescein) whereas the acceptor fluorophore in the 3' end was TAMRA (6-carboxytetramethylrhodamine). These oligonucleotides (Table 1) and ds26 (5'-CAATCGGATCGAATTCGATCCGATTG) were purchased from Eurogentec as dried samples and were dissolved with doubly deionized water. Stock solutions of 100 µM double-labelled oligonucleotides were stored at -20 °C. All the oligonucleotides were prepared by dissolving the stock solutions in annealing buffer consisting of 90 mM LiCl, 10 mM lithium cacodylate (LiCaC) and 10 mM KCl at pH = 7.2 except for F21RT prepared in 99 mM LiCl, 10 mM LiCaC and 1 mM KCl at pH = 7.2. The resulting solutions were heated at 90 °C during 5 minutes and then slowly cooled to room temperature. Oligonucleotide strands concentration were spectrophotometrically determined at λ = 260 nm using the absorptivity coefficients provided by the manufacturer. In the measures with DNA

View Article Online
DOI: 10.1039/D0DT02125C

polynucleotide, DNA was from calf thymus (ctDNA). It was purchased by Sigma as the highly polymerized sodium salt, shortened to ca. 500 base pairs and standardized as for molar concentration in base pairs of water solutions according to a standard procedure.[54]

Table 1. Sequences and Topologies of the double-labelled oligonucleotides used in this work

Name	Sequence (5'— 3')	Topology
F21T	FAM-GGGTTAGGGTTAGGGTTAGGG-TAMRA	Doubly labelled 3-tetrad Hybrid DNA G-quadruplex of human telomere
F21RT	FAM-GGGUUAGGGUUAGGGUUAGGG-TAMRA	Doubly labelled 3-tetrad Parallel RNA G-quadruplex of human telomere
F25CebT	FAM-AGGGTGGGTGTAAGTGTGGGTGGGT-TAMRA	Doubly labelled 3-tetrad Parallel DNA G-quadruplex of human minisatellite
F21CTAT	FAM-GGGCTAGGGCTAGGGCTAGGG-TAMRA	Doubly labelled 3-tetrad Antiparallel DNA G-quadruplex of human telomere
FmycT	FAM-TTGAGGGTGGGTAGGGTGGGTAA-TAMRA	Doubly labelled 3-tetrad Parallel DNA G-quadruplex of c-myc promoter
FBom17T	FAM-GGTTAGGTTAGGTTAGG-TAMRA	Doubly labelled 2-tetrad Antiparallel DNA G-quadruplex of *Bombyx* telomere
FTBAT	FAM-GGTTGGTGTGGTTGG-TAMRA	Doubly labelled 2-tetrad Antiparallel DNA G-quadruplex of Thrombin binding aptamer
FdxT	FAM-TATAGCTAT-hexaethyleneglycol-TATAGCTATA-TAMRA	Doubly labelled Intramolecular duplex

FRET Melting Assay was performed in a real time Polymerase Chain Reaction (7500 Fast Real Time PCR, Applied Biosystems) with the oligonucleotides described in Table 1 according to a procedure previously described.[55] Samples containing 0.2 µM oligonucleotide in the absence and in the presence of different concentrations of Zn(II) complexes were prepared in 96-well plates and scanned from 25 to 95°C at 1°C/min. The emission of FAM and TAMRA were measured during the denaturation in labelled oligonucleotide.The stabilisation induced by the Zn(II) complexes was calculated as the difference between the mid-transition temperature of the oligonucleotide (ΔTm) with and without the drug.

In FRET Melting Competition experiments samples were prepared with 0.2 µM of F21T, 5 µM of the Zn complexes and a 10, 25 and 50 excess of the DNA duplex competitor ds26 respecting the G4. The experiment were conducted under the same conditions as the FRET Melting Assay previously described.

Fluorescence measurements were performed with a Shimadzu Corporation RF-5301PC spectrofluorometer (Duisburg, Germany) and spectrophotometric measurements were performed with a Hewlett-Packard 8453A (Agilent Technologies, Palo Alto, CA) photodiode array

View Article Online
DOI: 10.1039/D0DT02125C

spectrophotometer. Titrations were carried out by adding increasing amounts of Tel22 to the Zn complexes in a 1 cm path-lenght cells at 25 °C.

Time correlated single photon counting (TCSPC) measurements were carried out for the fluorescence decay of the Zn complexes. The equipment used was FLS980 (Edinburgh Instruments). Photo excitation was made with a EPL 325 pulse diode laser. The data collected were analysed by FAST 3.4.0 software.

Isothermal titration calorimetry (ITC) experiments were performed at 25 °C using a Nano ITC (TA Instruments, Newcastle, USA). 25 injections of 2 µL of the Zn complexes were injected into the calorimetric cell containing the Tel22 solution with a stirring speed of 250 rpm. Prior to use, all solutions were degassed during 30 minutes in the degassing station (TA Instruments, Newcastle, USA) to avoid bubbles formation. Control experiments were carried out to determine the contribution of the heat of dilution of the Zn complexes and rule out the presence of aggregation processes. The obtained thermograms (integrated area of the peak/mole of injectant *versus* drug/Tel22 ratio) were fitted with Nanoanalyze software by a "two-site model" since the "one-site model" was insufficient to fit the data suitably.

Circular dichroism (CD) measurements were performed with a MOS-450 Biologic spectrophotometer (Bio-Logic SAS, Claix, France), fitted with 1.0 cm path-length cells. Titrations were carried out at 25 °C by adding increasing amounts of the dye to the Tel22 solution.

SW480 cells were cultured in Dulbecco's Modified Eagle's Medium (DMEM), supplemented with 10% FBS and 1% amphotericin-penicillin-streptomycin solution (all from Sigma Aldrich) and incubated in a humid atmosphere at 37 °C under 5% CO_2 atmosphere.

As to cytotoxicity studies, approximately 5×10^3 SW480 colon adenocarcinoma cells were cultured in 200 µL DMEM (Dulbecco's Modified Eagle Medium) per well and allow to proliferate at 37 °C and 5% CO_2. After 24h of incubation, the cells were exposed to different concentrations of the Zn complexes and incubated for other 48 h. Cisplatin was used as positive control. Then, cells were incubated with 100 µL of MTT (3-(4,5-dimethyltiazol-2-yl)-2,5-diphenyltetrazoliumbromide) (Sigma Aldrich) dissolved in culture medium (500 mg/ml) for a further period of 3 hours. After that, 100 µL of solubilizing solution (10% SDS, 0.01 M HCl) were added to each well and plates were incubated for 18 h at 37 °C. Formazan absorption was read at 590 nm in a microplate reader (Cytation 5 Cell Imaging Multi-Mode Reader - Biotek Instruments, USA). The IC_{50} values were calculated from cell survival data using nonlinear regression of the GraphPadPrism Software Inc. (version 6.01) (USA). Four replicates per dose were included and the reported IC_{50} values are the mean of at least two independent experiments.

For bioimaging experiments, SW480 cells were seeded in 96-well plate at a density of 1×10^4 cells/well in 200 µL DMEM without phenol red and allow to adhere for 24h at 37 °C and 5% CO_2. Then, cells were treated with the Zn complexes and 2 µM of Hoechst33258 and incubated at 37 °C under 5% CO_2 atmosphere for a short period of time. Finally, cells were visualized in a Cytation 5

View Article Online
DOI: 10.1039/D0DT02125C

Cell Imaging Multi-Mode Reader (Biotek Instruments, USA) in phase contrast, blue and orange fluorescence emission with a 20× objective.

For cellular uptake experiments, SW480 cells were seeded at a density of 1×10^6 cells/well in 6-well plates and grown for 24 h. Then, cells were exposed to 10 µM of the studied Zn complexes during 4 h. Cells were washed three times with DPBS (Dulbecco's Phosphate Buffered Saline) and then harvested. The pellets were resuspended in 1 mL of DPBS and 10 µL were used to count cells. Then, cells were centrifuged again and the pellet used for nuclear fragmentation as previously described.[56] The extracts were digested for ICP-MS (Inductively Coupled Plasma Mass Spectrometry) with 65% HNO_3 during 24 h. Finally, solutions were analysed in a 8900 ICP-MS (Agilent Technologies). Data are reported as the mean the standard deviation (n=3).

RESULTS AND DISCUSSION

Synthesis and characterization of the new Zn(II) terpyridine derivatives

The synthesis of ligands **L1**,[50] **L2**[51,52] and **L3**[51] was performed as described in the literature (see SI). The ligands were made to react with zinc salts in dichloromethane/acetonitrile (1:1) solutions and precipitates were obtained with yields in the range 72–85%. The reaction of $ZnCl_2$ with **L1**-**L3** (1:1 ratio) gave rise to complexes **1Cl**-**3Cl** (see Scheme 1). **2Cl**[53] was previously described although the NMR data were not provided. A five-coordination was found for this complex in the structure solved by X-ray diffraction and this was also the case for other [Zn(4R-tpy)Cl_2] derivatives.[44,46,57] Thus, the coordination of the three N atoms of the tpy ligands and the two chlorides is proposed for **1Cl** and **3Cl**. When $Zn(NO_3)_2\cdot 6H_2O$ was made to react with ligands **L1** and **L2** (1:1 ratio) the corresponding nitrato complexes **$1NO_3$** and **$2NO_3$** were formed. In similar derivatives of the type [Zn(4R-tpy)$(NO_3)_2$] a monodentate coordination for the two nitrate groups is found[43,58,59] and thus the same situation is proposed for **$1NO_3$** and **$2NO_3$**. Considering the lower cytotoxicity of **$1NO_3$** and **$2NO_3$** as compared to **1Cl** and **2Cl** (see below), we decided, in the case of ligand **L3**, to synthesize the complex [Zn(**L3**)$_2$]$(NO_3)_2$, **$3(L)_2$**, using a Zn:**L3** ratio of 1:2. Thus, a complex with a different geometry and an increased positive charge can be tested in the biological studies. A distorted octahedral structure is proposed based in previous reports of similar derivatives as [Zn(**L1**)$_2$]$(NO_3)_2$[60] or [Zn(tolyl-tpy)$_2$]$(PF_6)_2$.[48]

View Article Online
DOI: 10.1039/D0DT02125C

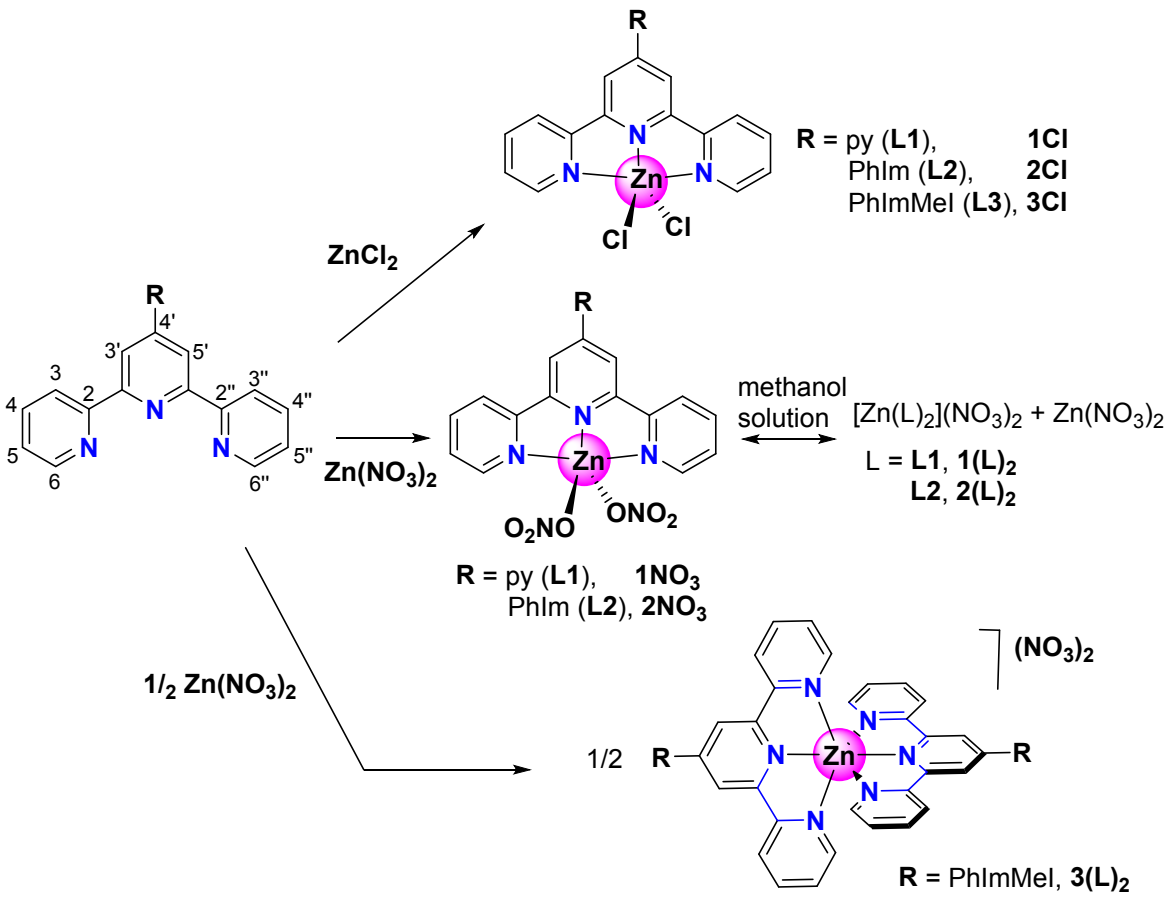

Scheme 1. Synthesis of the Zn(II) terpyridine derivatives and atom numbering scheme (see Figure 1 for the substituents on the ligands).

The Zn complexes were characterized by elemental analysis, FAB+ spectrometry and ^{1}H NMR spectroscopy (CD_3OD). In the FAB+ spectra, peaks corresponding to the loss of anions, including I^- in the case of complexes with **L3,** were detected. The ^{1}H NMR spectra of the ligands in the same solvent was registered for the sake of comparison (see SI). The assignment of the ^{1}H NMR resonances was done using both ^{1}H-^{1}H COSY spectra and bibliographic information[51] (see SI for the spectra and for an explanation about the general pattern of the ^{1}H NMR resonances). Symmetric ligands were observed in all complexes. In the case of the chloride derivatives, the resonances were shifted to lower field with respect to the free ligands. In the octahedral complex **3(L)$_2$**, a strong shielding of the $H^{6,6''}$ (1 ppm) and $H^{5,5''}$ signals (0.4 ppm) with respect **3Cl** occurs. This fact, already observed for other $[Zn(R\text{-}tpy)_2]^{2+}$ complexes,[57] should be due to the effect of the ring current of the other ligand of the complex. The nitrate complexes **1NO$_3$** and **2NO$_3$** exhibited in CD_3OD solution a process of partial disproportionation and a partial formation of the species **1(L)$_2$** or **2(L)$_2$** according to the equilibrium reflected in eq. 1 and Scheme 1, previously observed for other nitrate terpyridine Zn complexes.[57] As expected, the strong shielding of the $H^{6,6''}$ and $H^{5,5''}$ signals was observed for **1(L)$_2$** and **2(L)$_2$**.

View Article Online
DOI: 10.1039/D0DT02125C

$$2\ [Zn(NO_3)_2(L)] \leftrightarrow [Zn(L)_2](NO_3)_2 + Zn(NO_3)_2 \quad \text{(eq. 1)}$$

The ratio of the species in CD_3OD solution was the following: **$1NO_3$:$1(L)_2$** = 66:33 and **$2NO_3$:$2(L)_2$** = 69:31. It was decided to determine this ratio in the case of ligand **L3** and it was registered a solution of **L3** and $Zn(NO_3)_2$ in a 1:1 ratio. In this case, the ratio of **$3NO_3$:$3(L)_2$** was 82:18. The lower abundance of the octahedral complex in the case of **L3** may be due to the tetra positive charge of **$3(L)_2$**. It is noticeable the high influence of the stoichiometry and geometry of the complex on the position of the proton signals. In Figure S9 it is observed the similarity between the **3Cl** and **$3NO_3$** resonances and the clear difference with those of **$3(L)_2$**. It is interesting to note that both in **L3** and in their complexes, the signal for H^a of the imidazolyl ring is not observed, a fact that should be due to the deuteration of this proton in CD_3OD. The acidity of this proton should be enhanced by the methylation of this ring.

A clear effect of the initial concentration of **$1NO_3$** on the **$1NO_3$:$1(L)_2$** ratio was found (see Table 2 and Figure S10). This ratio did not change from 4.54 to 0.9 mM but at lower concentrations, the amount of **$1(L)_2$** was reduced and at 0.1 mM the unique species observed was **$1NO_3$**. Some changes in the chemical shifts are observed for **$1NO_3$** in this 0.1 mM solution. However, it is necessary to take into account that in compounds with terpy ligands, it is usual to observe modifications in chemical shifts when diluting due to the disappearance of weak interactions as π–π stacking. For example, π–π stacking has been found by X-ray diffraction in several terpyridine complexes of Zn.[61] The low field shifting of $H^{6,6''}$ may be due to the reduction of π–π stacking that could affect more strongly to these protons. In any case, an effect of partial ligand dissociation (free ligand in equilibrium with **$1NO_3$**) cannot be excluded at low concentrations of the complex.

Table 2. Percentage of **$1NO_3$** and **$1(L)_2$** in CD_3OD^a at different initial concentrations of **$1NO_3$.**

$[1NO_3]_0$ (mM)	**$1NO_3$ (%)**	**$1(L)_2$ (%)**
4.54	66	34
2.72	66	34
0.9	66	34
0.54	68	32
0.46	71	29
0.39	73	27
0.30	75	25
0.25	79	21
0.21	80	20
0.1	100	0

[a] Determined by ^1H NMR.

Thus, at the concentrations used for the biological studies (bellow 0.1 mM), it is expected that the octahedral derivatives will not be present for the compounds **$1NO_3$** and **$2NO_3$**.

Cytotoxicity

View Article Online
DOI: 10.1039/D0DT02125C

The cytotoxicity of all the synthesized Zn(II) complexes was studied in colon adenocarcinoma cells (SW480) by means of the MTT assay. The obtained half maximal inhibitory concentrations (IC_{50} values) after 48 h of exposure are collected in Table 3. Some conclusions regarding structure-activity relationship (SAR) studies can be extracted. On the one hand, there is strong influence of the leaving group in cytotoxicity, since the complexes bearing chloride are more cytotoxic that their analogues with nitrate. On the other hand, the substituent in the 4' position of the terpyridine ligand central ring also plays a role, since when comparing the chloride complexes, the most cytotoxic is **3Cl**, containing L3 ligand. In addition, the methyl group and/or the positive charge of the imidazole moiety provides **3Cl** complex with an antiproliferative activity comparable to that of the well-known anticancer agent cisplatin (CDDP). Interestingly, the addition of another terpyridine derivative results in a decrease of the cytotoxicity to the half. Therefore, the most interesting complex in terms of cytotoxicity is **3Cl.**

Table 3. IC_{50} values of the Zn complexes in SW480 cells within 48 h of incubation period.

	1Cl	**1NO_3**	**2Cl**	**2NO_3**	**3Cl**	**3$(L)_2$**	**CDDP**
IC_{50}, μM	34 ± 2	114 ± 5	29 ± 2	63 ± 4	17 ± 3	38 ± 1	20 ± 2

FRET Melting Assay

The G4 binding ability of the synthesized Zn complexes was investigated by FRET Melting Assay employing several oligonucleotides doubly labelled with FAM (F) and TAMRA (T) fluorophores. The set of used sequences are able to adopt different G4 topologies such as parallel (F21RT, F25CebT, FmycT), antiparallel (F21CTAT, FBom17T, FTBAT) and hybrid (F21T) structures. The aim was to study not only the ability to thermally stabilize G4 but also to test their potential selectivity towards one particular G4 conformation. The gathered results (Figure 2) revealed that among the ligands, only L2 and L3 are able to thermally stabilized G4 being the thermal stabilization induced by L2 negligible in all the tested G4 with the exception of F21T and F21RT. L3 is the most stabilizing ligand, but stabilizes G4 structures in a less extent than whatever of the synthesised complexes. All the synthesized complexes were able to bind G4 and the substituent in the 4' position of the terpyridine central ring had a great influence on the thermal stabilization since as greater was the extension, the larger was the ΔTm ($Tm_{Zn\ complex/Oligo} - Tm_{Oligo}$). The greatest stabilization was observed for the Zn complexes bearing **L3**, **3Cl** and **3$(L)_2$**, probably due to their extra positive charge. By contrast, ΔTm was not influenced by the leaving group –Cl or –NO_3.

View Article Online
DOI: 10.1039/D0DT02125C

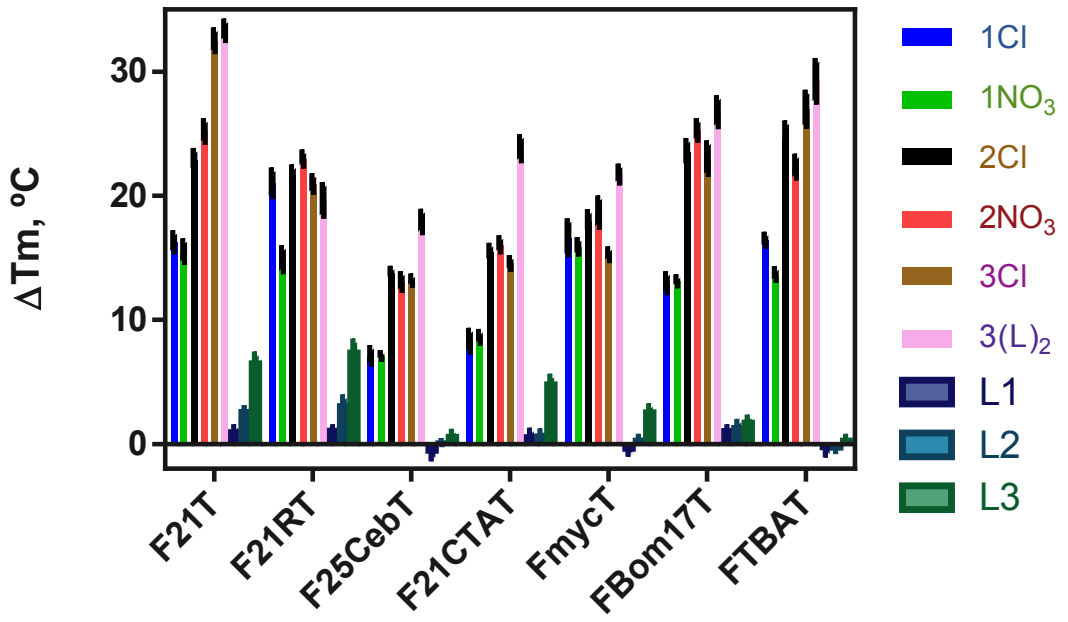

Figure 2. ΔTm ($Tm_{Zn\ complex/Oligo} - Tm_{Oligo}$) of several G4 oligonucleotides in the presence of 10 μM of the studied ligands and their Zn complexes. C_{Oligo} = 0.2 μM, I = 0.11 M (90 mM LiCl, 10 mM KCl, 10 mM LiCaC) and pH 7.2.

Thus, in the light of cytotoxicity and FRET melting experiments, the Zn complexes bearing **L3** as terpyridine derivative, **3Cl** and **3(L)$_2$**, are the most interesting and they were selected for further studies to enlighten their potential biological activity.

*Stability and aquation studies for **3Cl** and **3(L)$_2$** in D_2O*

Firstly, the stability and potential aquation of the selected terpyridine derivatives, **3Cl** and **3(L)$_2$**, was performed. It was observed by ^{1}H NMR studies that **3(L)$_2$** was stable in D_2O solution (one day, Figure S19) and no other species nor free ligand **L3** were detected. When **3Cl** was solved in D_2O (4.7 mM), narrow signals of **3(L)$_2$** were instantaneously observed in the ^{1}H NMR spectrum along with other broad signals that should correspond to aquation products in mutual interchange ($[Zn(\mathbf{L3})Cl_{2-n}(D_2O)_n]Cl_n$, n = 1,2, see Figure S20). Considering that **3(L)$_2$** was not formed in the methanolic solution of **3Cl**, it is proposed that **3(L)$_2$** is formed from the aquation products (see eq. 2). This solution did not change after one day. Taking into account that the biological experiments were performed in the presence of 0.1 M of chloride, the evolution of the previous solution in the presence of the 0.1M KCl was analysed. A precipitate was formed, and the solution had not enough concentration to get a proper ^{1}H NMR spectrum. Thus, it is possible to assure that **3(L)$_2$** is not present in this medium (**3(L)$_2$** is water soluble, Figure S19). Consequently, the presence of an excess of chloride anions prevents the aquation process of **3Cl** and decrease its water solubility. It is

View Article Online
DOI: 10.1039/D0DT02125C

interesting to note that free ligand **L3** was not observed in the different experiments excluding its presence in the biological tests.

$$[Zn(\mathbf{L3})Cl_2] \underset{Cl^-}{\overset{D_2O}{\rightleftharpoons}} [Zn(\mathbf{L3})Cl_{2-n}(D_2O)_n]Cl_n \;(n = 1,2) \rightleftharpoons 1/2\,[Zn(\mathbf{L3})_2]Cl_2 + 1/2\,[Zn(D_2O)_6]Cl_2 \quad \text{(eq.2)}$$

3Cl **3(L)$_2$**

The stability and potential aggregation of **3Cl** and **3(L)$_2$** was also investigated in aqueous buffered solution by measuring their absorbance along time. After 24h no changes were observed in the recorded absorbance spectra (Figure S21) and both complexes fulfil Lambert Beer's law in the studied concentration range, which enable us to discard auto-aggregation phenomena (Figure S22).

Since both complexes are fluorescent molecules, their 3D fluorescence spectra were recorded: no appreciable difference between them was observed (Figure S23A and B). Time-correlated single photon counting (TCSPC) measurements were also performed and only small differences were observed in their emission lifetimes being τ = 5.2 and 5.4 ns for **3Cl** and **3(L)$_2$** respectively (Figure S23C).

*Interaction of G4 sequences with **3Cl** and **3(L)$_2$***

In order to complete the FRET Melting Assay results of Figure 2, the G4 binding ability of the free terpyrididine (**L3**), the mono (**3Cl**) and the bis-terpyridine (**3(L)$_2$**) derivatives (from now named as D), was evaluated at different complex concentrations, by employing the seven G4s previously described and an extra sequence able to form an intramolecular duplex (FdxT). A radar plot of the calculated ΔTm values enables an easy identification of a potential selectivity towards a specific G4 topology (Figure 3).[55] For instance, selectivity towards 2-tetrad over 3-tetrad quadruplexes has been previously described by our group for a perylene diimide derivative.[62] Here, **L3**, **3Cl** and **3(L)$_2$** were found to thermally stabilized G4s in a dose-dependent manner (Figure 3). Also, the thermal stabilization profiles showed that the hybrid conformation adopted by the human telomeric oligonucleotide (F21T) was stabilized in a greater extent than the parallel or antiparallel conformations in 3-tetrad and 2-tetrads G4s. In this regard, it should be noticed that the ligand behaves in a different way, since **L3** stabilizes the paralell RNA G4 (F21RT) as much as the hybrid F21T, followed by the antiparallel F21CTAT and then, negligible stabilization for other G4 sequences was observed. 7°C is the highest thermal stabilization induced by the ligand in the hybrid human telomeric G4, at the highest concentration (10 μM). This value is very low in comparison with the thermal stabilization induced by **3Cl** or **3(L)$_2$** (15°C and 18°C, respectively) at the lowest concentration (0.5 μM). Thus, there is a strong influence of the metal fragment on the stabilization of G4 structures. In addition, for the DNA human telomeric sequence, the saturation concentration was lower in the case of **3Cl** (2 μM) than in **3(L)$_2$** (> 5 μM), which indicated greater affinity of the former for F21T. This behaviour will be subsequently confirmed by FRET melting competition and ITC experiments. Interestingly, **3Cl** displayed no significant effect on the thermal stabilization of the intramolecular duplex (FdxT) whereas **3(L)$_2$** seemed to thermally stabilize it, pointing out a potential interaction of **3(L)$_2$** with duplex DNA.

View Article Online
DOI: 10.1039/D0DT02125C

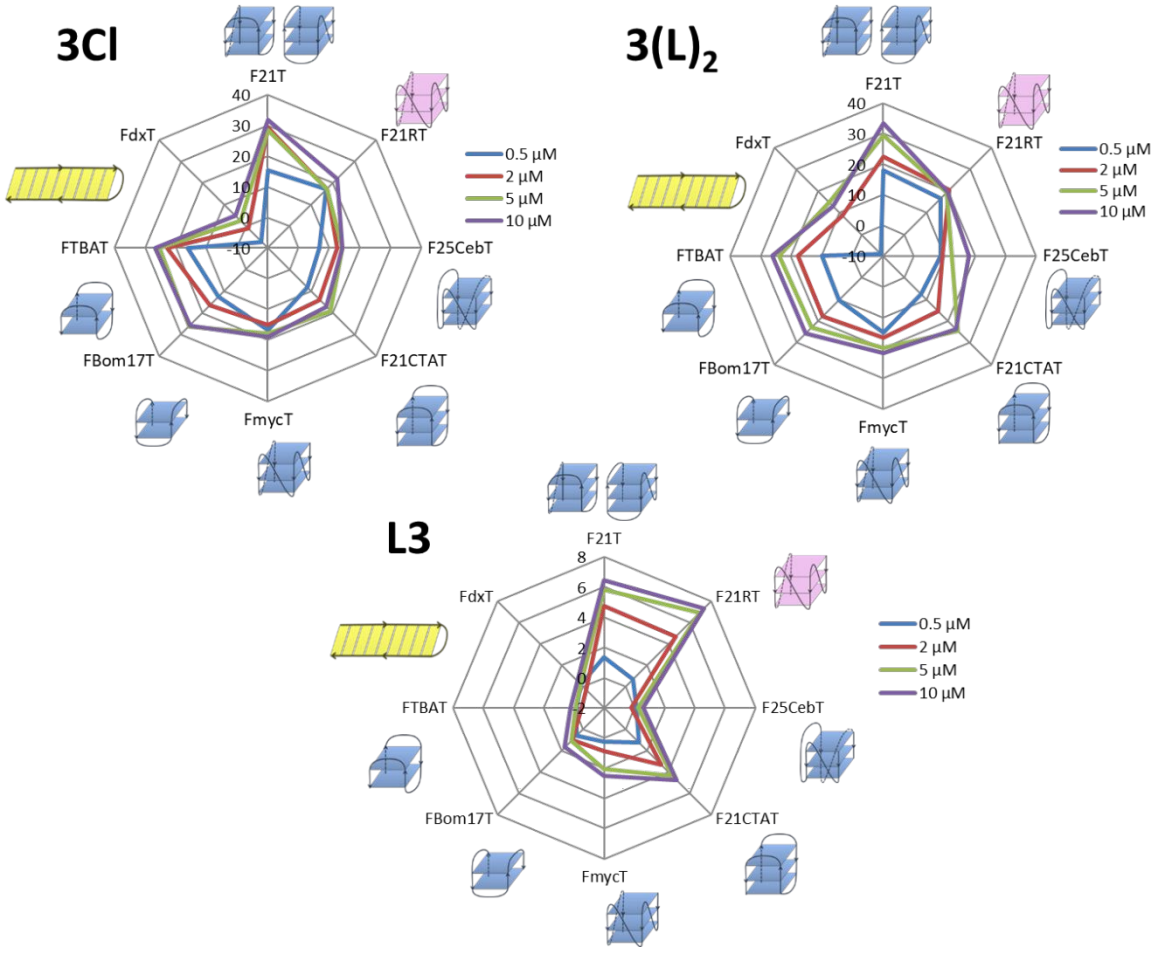

Figure 3. ΔTm Radar Plot of several oligonucleotides in the presence of different concentrations of **3Cl** (left) and **3(L)$_2$** (right) and **L3** (down). C_{Oligo} = 0.2 µM, I = 0.11 M (90 mM LiCl, 10 mM KCl, 10 mM LiCaC) and pH 7.2.

Selectivity towards G-quadruplex conformation

In order to shed some light on the selectivity of these Zn complexes towards G4s over duplex structures, FRET melting competition experiments were carried out at 5 µM of the Zn complexes with the most stabilized sequence (F21T) and different concentrations of a duplex (ds26) as competitor. From the comparison of the variations induced by the presence of the competitor, it can be deduced that the addition of other terpyridine moiety diminishes the selectivity towards G4 structures (Figure 4). Indeed, the thermal stabilization of the human telomeric sequence induced by **3Cl** suffers a slight variation at 50 fold excess of DNA double helix that may be considered negligible in comparison to the observed variation just at 25 fold excess for **3(L)$_2$**.

View Article Online
DOI: 10.1039/D0DT02125C

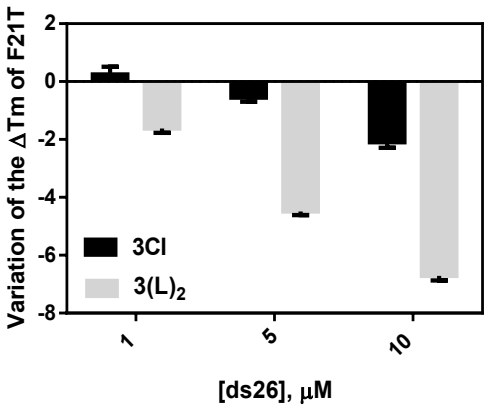

Figure 4. Variation of the ΔTm ($\Delta Tm_{competitor}$-$\Delta Tm_{w/o\ competitor}$) induced by 5 μM of **3Cl** or **3(L)$_2$** in the presence of different concentrations of competitor. C_{F21T} = 0.2 μM, I = 0.11 M (90 mM LiCl, 10 mM KCl, 10 mM LiCaC) and pH 7.2.

This behaviour confirms the results recorded in Figure 3, absence of FdxT interaction with **3Cl** and FdxT stabilization by **3(L)$_2$**.

To properly confirm the **3(L)$_2$** ability to bind to the DNA double helix, its interaction with ctDNA was studied by means of absorbance, fluorescence, circular dichroism (CD), viscosity and stopped flow techniques. From the fluorescence data, the Scatchard analysis (see eq 1SI and Figure S24) revealed that **3(L)$_2$** interacted with DNA double helix with an equilibrium binding constant of K_b = (2.3 ± 0.3) × 10^5 M^{-1} and site size n = 2.3. These values, together with CD (Figure S25A) and viscosity (Figure S25B) experiments, enlightened the presence of a binding mode which is a mixture of partial intercalation and groove binding. The binding was also studied by a kinetic approach; since the reaction between **3(L)$_2$** and DNA was fast, stopped-flow was necessary. The data pairs, reciprocal time constant, 1/τ versus **3(L)$_2$** concentration (Figure S26), indicated a two steps mechanism: a very fast pre-equilibrium leads to the formation of an intermediate that evolve to the final DNA/**3(L)$_2$** product. At this point, it can be concluded that **3(L)$_2$** does not display as much selectivity for G4 as **3Cl** does.

Human telomeric G-quadruplex interaction

As we see above, both **3Cl** and **3(L)$_2$** complexes are fluorescent in the working conditions. Upon addition of the human telomeric G4, Tel22, to the complexes solutions, a quenching effect is observed for both complexes being this effect more pronounced for **3Cl** than for **3(L)$_2$** (Figure 5). This behaviour could be easily related to the affinity of these Zn complexes towards Tel22 which is higher for **3Cl** than for **3(L)$_2$** (see below).

View Article Online
DOI: 10.1039/D0DT02125C

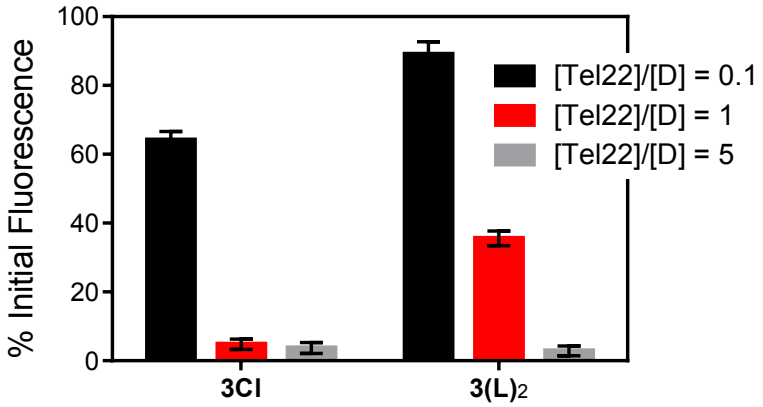

Figure 5. Percentage of initial fluorescence of the **3Cl** and **3(L)$_2$** complexes (D) in the presence of different amounts of Tel22. C_D = 1 µM, I = 0.11 M (90 mM LiCl, 10 mM KCl, 10 mM LiCaC), pH 7.2 and 25°C.

In order to quantify the affinity of the Zn complexes towards Tel22, fluorescence titrations were carried out. The fluorescence emission decay of both Zn complexes upon the addition of Tel22 (Figure 6) reinforcing the hypothesis that the complexes formed are not fluorescent. The binding isotherms are monophasic (insets Figure 6) and were analysed according to the Scatchard Equation (Eq 1SI and Fig. S27), the values achieved for the binding constants are (14.8 ± 0.6)×10^6 and (2.2 ± 0.1) ×10^6 M^{-1} for **3Cl** and **3(L)$_2$**, respectively.

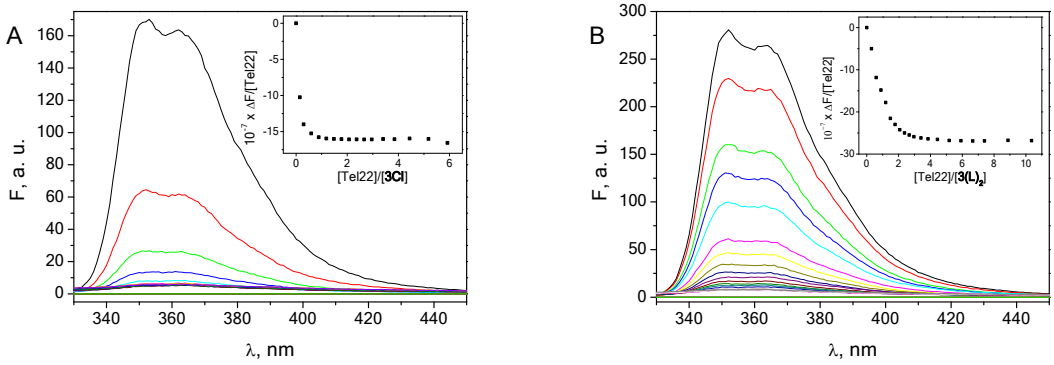

Figure 6. Fluorescence spectra recorded during the titration of **3Cl** (A) and **3(L)$_2$** (B) with Tel22. The insets are the binding isotherms at 340 nm. C_D = 1 µM, I = 0.11 M (90 mM LiCl, 10 mM KCl, 10 mM LiCaC), pH 7.2 and 25°C.

Absorbance titrations were also carried out. Interestingly, for both Zn complexes the recorded spectra showed a complex behaviour with a biphasic binding isotherm (Figure 7). In the first trend, there was a hypochromic effect when Tel22 was added to the Zn complex solution up to [Tel22]/[**3Cl**] = 0.15 and [Tel22]/[**3(L)$_2$**] = 0.32. Then, a hyperchromic effect occurred in both systems.

View Article Online
DOI: 10.1039/D0DT02125C

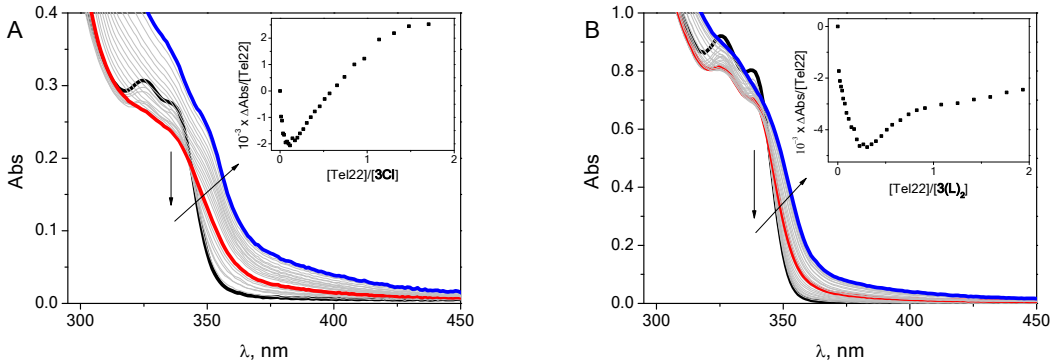

Figure 7. Absorbance spectra recorded during the titration of **3Cl** (A) and **3(L)$_2$** (B) with Tel22. The insets are the binding isotherms at 340 nm. The first branch goes from black to red solid line and the second trend from red to blue solid line. C_D = 26 µM, I = 0.11 M (90 mM LiCl, 10 mM KCl, 10 mM LiCaC), pH 7.2 and 25°C.

The biphasic pattern observed in absorbance binding isotherms revealed that the binding of these Zn complexes to Tel22 is not a simple process. The fact that only one process is observed by fluorescence titrations can be easily explained in the light of quenching experiments that evinced that products of the binding reactions are not fluorescent.

The existence of two different complexes as a function of the Tel22/Zn complex ratio was also confirmed by Isothermal Titration Calorimetry (ITC). This method has been reported as appropriate to determine the affinity of metal complexes interaction with G4 when more than one binding process is at work. [63,64,65] The thermograms corroborated the biphasic behaviour observed in absorbance titrations (Figure 8). The thermodynamic parameters obtained for the interaction of the Zn complexes with Tel22 by means of the "Multiple Sites" model are collected in Table 4. According to these data, all the binding processes are exothermic and the entropic component of process 1 is very high suggesting that the binding is entropically driven.

View Article Online
DOI: 10.1039/D0DT02125C

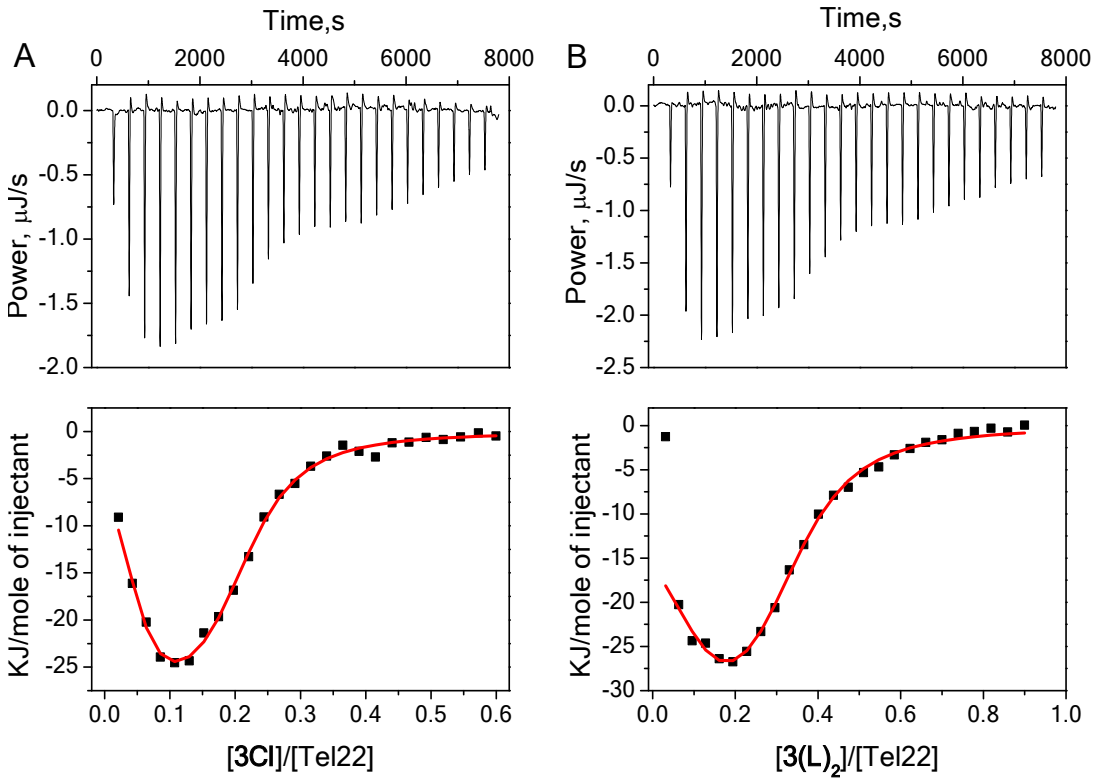

Figure 8. ITC continuous titrations of Tel22 with **3Cl** (A) and **3(L)$_2$** (B). C_{Tel22} = 52 µM, I = 0.11 M (90 mM LiCl, 10 mM KCl, 10 mM LiCaC), pH 7.2 and 25°C.

Table 4. Thermodynamic parameters of the interaction of the Zn complexes with the human telomeric G-quadruplex Tel22 at I = 0.11 M (90 mM LiCl, 10 mM KCl, 10 mM LiCaC), pH 7.2 and 25°C determined by the "Multiple Sites" model.

	3Cl/Tel22	**3(L)$_2$**/Tel22
10^{-6} K_1, M^{-1}	4.05 ± 0.83	0.45 ± 0.08
ΔH_1, kJ/mol	-2.73 ± 0.21	-3.01 ± 0.10
ΔS_1, J/mol·K	117.3	98.1
10^{-5} K_2, M^{-1}	1.84 ± 0.22	0.64 ± 0.12
ΔH_2, kJ/mol	-14.76 ± 0.41	-13.41 ± 0.32
ΔS_2, J/mol·K	51.3	47.4

To better study the effect of the Zn complexes on the Tel22 structure, circular dichroism titrations were carried out. It is known that Tel22 in K^+ solution adopts a hybrid conformation with a maximum at 290 nm and a shoulder at 270 nm. Unlike the reported changes in the CD spectra of other Zn

View Article Online
DOI: 10.1039/D0DT02125C

terpyridine derivatives that bind to G4 by external binding,[41] for these derivatives, there are no clear differences in the spectra when **3Cl** and **3(L)$_2$** are added to a Tel22 solution (Figure S28).

Even though both Zn complexes are able to interact with Tel22, only **3Cl** displays selectivity towards G4 over duplex structures. Moreover, both the fluorescence and ITC experiments had shown that the affinity of **3Cl** by human telomeric G4 is higher than that of **3(L)$_2$**. Both characteristics, high G4 selectivity and affinity, together with its high cytotoxicity, make **3Cl** a very interesting complex from a biological point of view.

Cellular Internalization

Once their ability as G4 ligands as well as their cytotoxicity are determined, one wonders whether they are internalized inside the cells and where they are mainly accumulated. To confirm their cellular internalization and taking advantage of their emission properties, the cellular uptake of both Zn complexes by colon adenocarcinoma cells was investigated firstly by fluorescence bioimaging. As it can be observed in Figure 9, both complexes were successfully internalized by SW480 cells within 30 minutes of exposition and they seemed to be localized mainly in the nucleus.

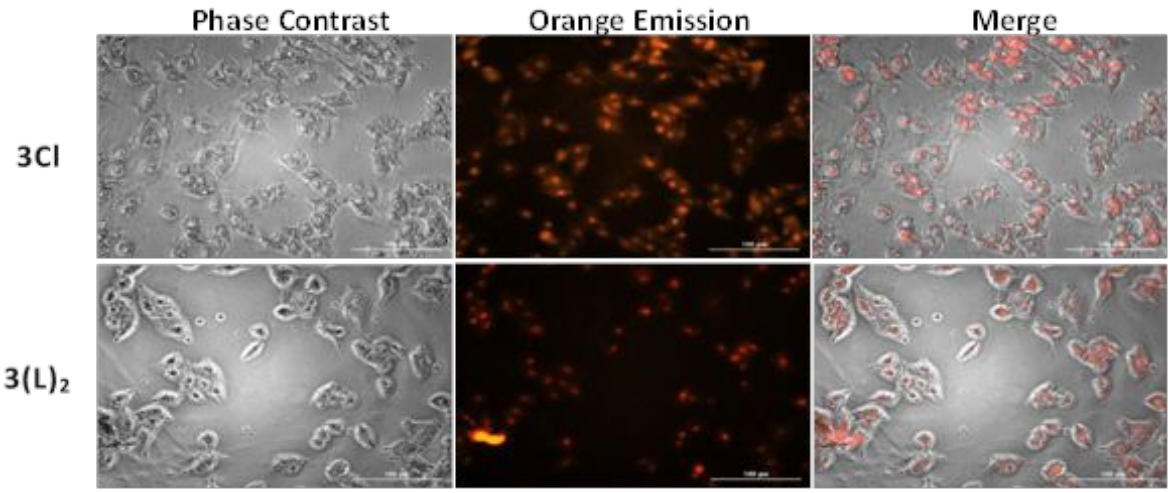

Figure 9. Images of SW480 cells treated with 10 μM of **3Cl** and **3(L)$_2$** during 30 minutes

To corroborate their nuclear localization, a specific nuclear probe (Hoechst33258) was employed. Interestingly, when SW480 cells are co-stained with Hoechst33258, small circular areas with orange emission are visualized inside the nucleus (Figure 10) suggesting nucleolus localization of the Zn complexes.

View Article Online
DOI: 10.1039/D0DT02125C

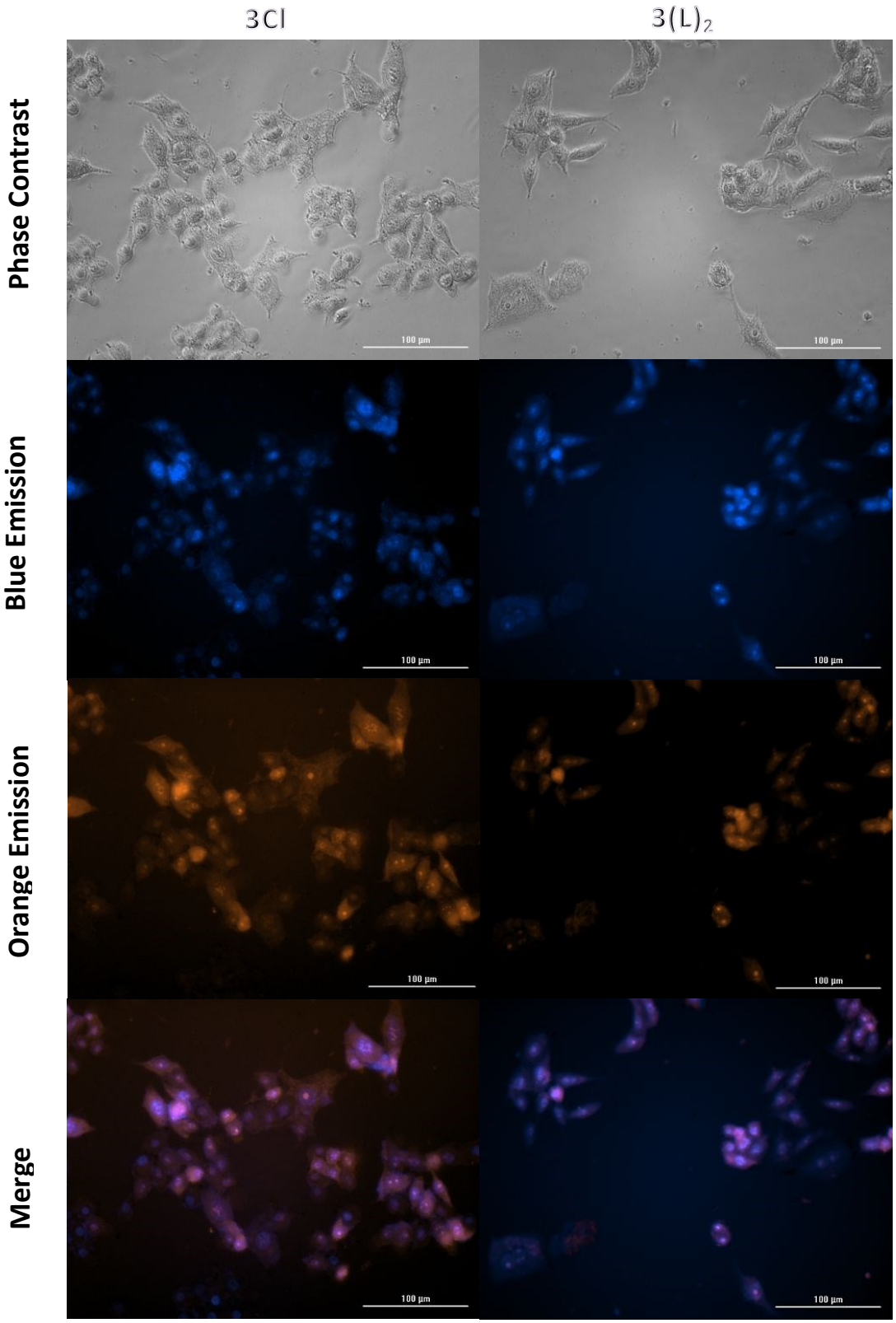

Figure 10. Images of SW480 cells treated with 5 µM of **3Cl** and **3(L)$_2$** and 2 µM of Hoechst33258 during 1h.

View Article Online
DOI: 10.1039/D0DT02125C

In an attempt to confirm these results, the cellular uptake of these Zn complexes was quantified by ICP-MS measurements. Untreated cells were included as control samples to enable endogenous Zn correction. The results collected in Figure 11 showed that both Zn complexes were more internalized by SW480 cells than cisplatin (CDDP). The cellular uptake of **3Cl** was greater than that of **3(L)$_2$** (Figure 11A) according to the observed cytotoxic activity (Table 3). Regarding subcellular localization, the majority of both Zn complexes were accumulated in the nucleus being only around a 9% in the cytoplasm. What is more, within the nucleus, the 85% of the Zn was accumulated in the nucleolus (Figure 11B) in good correlation with the previously observed fluorescence images. This subcellular localization is also the localization of Quarfloxin, a fluoroquinolone derivative with antineoplastic activity that binds to ribosomal DNA G-quadruplex and it is being evaluated in phase II clinical studies for the treatment of neuroendocrine carcinoma.[66]

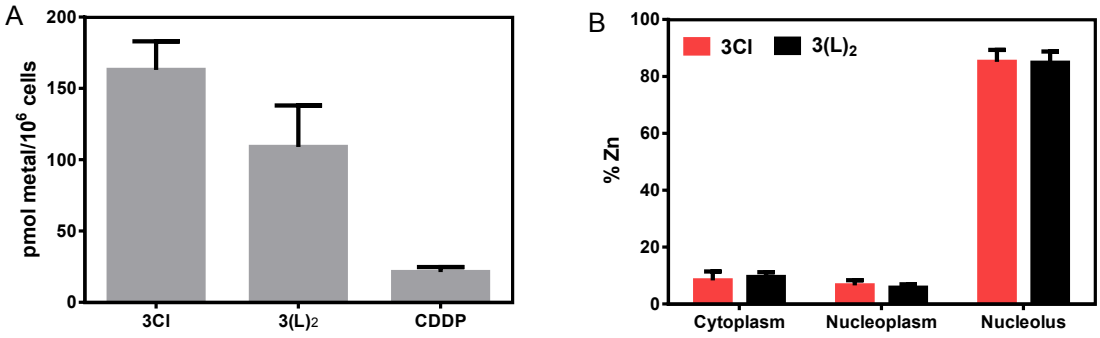

Figure 11. Metal accumulation inside SW480 cells treated with 10 µM of the metal complexes during 4h.

CONCLUSIONS

Six Zn(II) chloride or nitrate complexes with 4'-substituted terpyridine ligands were synthesized and characterized enabling some SAR conclusions. Firstly, the role played by the leaving group in terms of cytotoxicity is crucial being the complexes with chloride as leaving groups more cytotoxic that their analogues with nitrate. By contrast, the nature of the leaving groups does not seem to have a direct effect in G4 thermal stabilization. Another important conclusion is that the more extended is the substituent in the 4' position of the terpyridine ligand central ring, the higher is the cytotoxic effect and the G4 thermal stabilization. The complexes bearing **L3** with a methylated 4-(Imidazol-1-yl)phenyl substituent are the most stabilizing G4 ligands, probably due to their extra positive charges. Ligand release was not observed in the experimental conditions of the biological studies. FRET melting experiments had shown that **3(L)$_2$** is less selective than **3Cl** towards G4 structures not only because intramolecular dsDNA (FdxT) was stabilized to a greater extent by the former but also because dsDNA (ds26) results to be an efficient competitor for **3(L)$_2$**. The affinity of **3(L)$_2$** by natural

View Article Online
DOI: 10.1039/D0DT02125C

dsDNA (ctDNA) was determined by thermodynamic and kinetic experiments revealing a mixture of partial intercalation and groove binding as binding modes. Moreover, fluorescence and ITC experiments indicated greater affinity (higher binding constant) of **3Cl** than **3(L)$_2$** towards human telomeric G4 Tel22. We can then conclude that the most interesting complex in terms of affinity and selectivity towards human telomeric G4 Tel22 is **3Cl.**

The most interesting Zn complex in terms of cytotoxicity is also **3Cl** with an antiproliferative activity comparable to that of the well-known anticancer agent cisplatin (CDDP). Interestingly, the addition of another terpyridine derivative in **3(L)$_2$** results in a decrease of the cytotoxicity to the half. Both Zn complexes are better internalized than cisplatin by colon adenocarcinoma cells and they are successfully visualized inside the cells being mainly localized in the nucleolus.

Conflicts of interest. The authors declare that they have no conflict of interest.

ACKNOWLEDGEMENTS

The financial support of "la Caixa" Foundation (LCF/PR/PR12/11070003), Ministerio de Ciencia, Innovación y Universidades-FEDER (RTI2018-102040-B-100 and RTI2018-100709-B-C21) and Junta de Castilla y León-FEDER (BU305P18) is gratefully acknowledged. N.B, T.B and B.G are grateful to COST Action CA18202 for networking support.

REFERENCES

1 J. T. Davis, *Angew. Chemie Int. Ed.*, 2004, **43**, 668–698.
2 S. Burge, G. N. Parkinson, P. Hazel, A. K. Todd and S. Neidle, *Nucleic Acids Res.*, 2006, **34**, 5402–5415.
3 D. Bhattacharyya, G. M. Arachchilage and S. Basu, *Front. Chem.*, 2016, **4**, 1–14.
4 V. S. Chambers, G. Marsico, J. M. Boutell, M. Di Antonio, G. P. Smith and S. Balasubramanian, *Nat. Biotechnol.*, 2015, **33**, 877–881.
5 A. Shivalingam, M. A. Izquierdo, A. Le Marois, A. Vyšniauskas, K. Suhling, M. K. Kuimova and R. Vilar, *Nat. Commun.*, 2015, **6**, 8178.
6 H. J. Lipps and D. Rhodes, *Trends Cell Biol.*, 2009, **19**, 414–422.
7 D. Rhodes and H. J. Lipps, *Nucleic Acids Res.*, 2015, **43**, 8627–8637.
8 M. Metifiot, S. Amrane, S. Litvak and M. L. Andreola, *Nucleic Acids Res.*, 2014, **42**, 12352–12366.
9 N. Maizels, *EMBO Rep.*, 2015, **16**, 910–922.
10 S. Neidle, *J. Med. Chem.*, 2016, **59**, 5987–6011.
11 S. Neidle, *Nat. Rev. Chem.*, 2017, **1**, 1–10.
12 R. Hänsel-Hertsch, M. Di Antonio and S. Balasubramanian, *Nat. Rev. Mol. Cell Biol.*, 2017, **18**, 279–284.
13 N. Saranathan and P. Vivekanandan, *Trends Microbiol.*, 2019, **27**, 148–163.
14 D. Monchaud and M. P. Teulade-Fichou, *Org. Biomol. Chem.*, 2008, **6**, 627–636.
15 M. Zuffo, A. Guédin, E. D. Leriche, F. Doria, V. Pirota, V. Gabelica, J. L. Mergny and M. Freccero, *Nucleic Acids Res.*, 2018, **46**, e115.
16 S. N. Georgiades, N. H. Abd Karim, K. Suntharalingam and R. Vilar, *Angew. Chemie - Int. Ed.*, 2010, **49**, 4020–4034.

View Article Online
DOI: 10.1039/D0DT02125C

17 Q. Cao, Y. Li, E. Freisinger, P. Z. Qin, R. K. O. Sigel and Z. W. Mao, *Inorg. Chem. Front.*, 2017, **4**, 10–32.
18 H. Hofmeier and U. S. Schubert, *Chem. Soc. Rev.*, 2004, **33**, 373–399.
19 E. C. Constable, *Chem. Soc. Rev.*, 2007, **36**, 246–253.
20 F. Puntoriero, S. Campagna, A. M. Stadler and J. M. Lehn, *Coord. Chem. Rev.*, 2008, **252**, 2480–2492.
21 F. A. Murphy, S. Suarez, E. Figgemeier, E. R. Schofield and S. M. Draper, *Chem. - A Eur. J.*, 2009, **15**, 5740–5748.
22 J. P. Collin, S. Guillerez, J. P. Sauvage, F. Barigelletti, L. Flamigni, L. De Cola and V. Balzani, *Inorg. Chem.*, 1991, **30**, 4230–4238.
23 Y. H. Lee, E. Kubota, A. Fuyuhiro, S. Kawata, J. M. Harrowfield, Y. Kim and S. Hayami, *Dalt. Trans.*, 2012, **41**, 10825–10831.
24 G. Chelucci and R. P. Thummel, *Chem. Rev.*, 2002, **102**, 3129–3170.
25 I. Eryazici, C. N. Moorefield and G. R. Newkome, *Chem. Rev.*, 2008, **108**, 1834–1895.
26 E. Largy, F. Hamon, F. Rosu, V. Gabelica, E. De Pauw, A. Guédin, J. L. Mergny and M. P. Teulade-Fichou, *Chem. - A Eur. J.*, 2011, **17**, 13274–13283.
27 S. Gama, I. Rodrigues, F. Mendes, I. C. Santos, E. Gabano, B. Klejevskaja, J. Gonzalez-Garcia, M. Ravera, R. Vilar and A. Paulo, *J. Inorg. Biochem.*, 2016, **160**, 275–286.
28 Y. Li, M. Cheng, J. Hao, C. Wang, G. Jia and C. Li, *Chem. Sci.*, 2015, **6**, 5578–5585.
29 K. Suntharalingam, A. J. P. White and R. Vilar, *Inorg. Chem.*, 2009, **48**, 9427–9435.
30 A. Savić, T. Marzo, F. Scaletti, L. Massai, G. Bartoli, R. Hoogenboom, L. Messori, R. Van Deun and K. Van Hecke, *BioMetals*, 2019, **32**, 33–47.
31 H. Bertrand, S. Bombard, D. Monchaud, E. Talbot, A. Guédin, J. L. Mergny, R. Grünert, P. J. Bednarski and M. P. Teulade-Fichou, *Org. Biomol. Chem.*, 2009, **7**, 2864–2871.
32 V. S. Stafford, K. Suntharalingam, A. Shivalingam, A. J. P. White, D. J. Mann and R. Vilar, *Dalt. Trans.*, 2015, **44**, 3686–3700.
33 K. Suntharalingam, A. J. P. White and R. Vilar, *Inorg. Chem.*, 2010, **49**, 8371–8380.
34 Y. Cherasse and Y. Urade, *Int. J. Mol. Sci.*, , DOI:10.3390/ijms18112334.
35 A. S. Prasad, *Adv. Nutr.*, 2013, **4**, 176–190.
36 T. Hara, T. aki Takeda, T. Takagishi, K. Fukue, T. Kambe and T. Fukada, *J. Physiol. Sci.*, 2017, **67**, 283–301.
37 C. T. Chasapis, C. A. Spiliopoulou, A. C. Loutsidou and M. E. Stefanidou, *Arch. Toxicol.*, 2012, **86**, 521–534.
38 J. I. Dupont, K. L. Henderson, A. Metz, V. H. Le, J. P. Emerson and E. A. Lewis, *Biochim. Biophys. Acta - Gen. Subj.*, 2016, **1860**, 902–909.
39 A. D. Beniaminov, R. A. Novikov, O. K. Mamaeva, V. A. Mitkevich, I. P. Smirnov, M. A. Livshits, A. K. Shchyolkina and D. N. Kaluzhny, *Nucleic Acids Res.*, 2016, **44**, 10031–10041.
40 R. Bonsignore, F. Russo, A. Terenzi, A. Spinello, A. Lauria, G. Gennaro, A. M. Almerico, B. K. Keppler and G. Barone, *J. Inorg. Biochem.*, 2018, **178**, 106–114.
41 J. Jiang, J. Li, C. Liu, R. Liu, X. Liang, Y. Zhou, L. Pan, H. Chen and Z. Ma, *J. Biol. Inorg. Chem.*, 2020, **25**, 311–324.
42 H. Bertrand, D. Monchaud, A. De Cian, R. Guillot, J. L. Mergny and M. P. Teulade-Fichou, *Org. Biomol. Chem.*, 2007, **5**, 2555–2559.
43 H. H. Zou, J. G. Wei, X. H. Qin, S. G. Mo, Q. P. Qin, Y. C. Liu, F. P. Liang, Y. L. Zhang and Z. F. Chen, *Medchemcomm*, 2016, **7**, 1132–1137.
44 Z. Ma, Y. Cao, Q. Li, M. F. C. Guedes da Silva, J. J. R. Fraústo da Silva and A. J. L. Pombeiro, *J. Inorg. Biochem.*, 2010, **104**, 704–711.
45 W. Chu, Y. Wang, S. Liu, X. Yang, S. Wang, S. Li, G. Zhou, X. Qin, C. Zhou and J. Zhang,

View Article Online
DOI: 10.1039/D0DT02125C

Bioorganic Med. Chem. Lett., 2013, **23**, 5187–5191.

46 S. Wang, W. Chu, Y. Wang, S. Liu, J. Zhang, S. Li, H. Wei, G. Zhou and X. Qin, *Appl. Organomet. Chem.*, 2013, **27**, 373–379.

47 X. Liang, J. Jiang, X. Xue, L. Huang, X. Ding, D. Nong, H. Chen, L. Pan and Z. Ma, *Dalt. Trans.*, 2019, **48**, 10488–10504.

48 Q. Jiang, J. Zhu, Y. Zhang, N. Xiao and Z. Guo, *BioMetals*, 2009, **22**, 297–305.

49 C. Hounsou, L. Guittat, D. Monchaud, M. Jourdan, N. Saettel, J. L. Mergny and M. P. Teulade-Fichou, *ChemMedChem*, 2007, **2**, 655–666.

50 J. Wang and G. Hanan, *Synlett*, 2005, **2005**, 1251–1254.

51 S. K. Gupta and J. Choudhury, *Dalt. Trans.*, 2014, **44**, 1233–1239.

52 C. X. Wang, L. Li, W. T. Yu, J. X. Yang and L. Y. Wu, *Acta Crystallogr. Sect. E Struct. Reports Online*, 2006, **62**, 246–248.

53 W. W. Fu, Q. Huang, S. T. Liu, W. J. Wu, J. R. Shen and S. H. Li, *Russ. J. Coord. Chem. Khimiya*, 2017, **43**, 670–678.

54 T. Biver, N. Eltugral, A. Pucci, G. Ruggeri, A. Schena, F. Secco and M. Venturini, *Dalt. Trans.*, 2011, **40**, 4190.

55 A. De Rache and J. L. Mergny, *Biochimie*, 2015, **115**, 194–202.

56 Z. F. Li and Y. W. Lam, in *The Nucleus. Methods in Molecular Biology (Methods and Protocols), vol 1228.*, Humana Press, New York, NY, 2015, pp. 35–42.

57 J. R. Jeitler, M. M. Turnbull and J. L. Wikaira, *Inorganica Chim. Acta*, 2003, **351**, 331–344.

58 M. Wałęsa-Chorab, A. R. Stefankiewicz, D. Ciesielski, Z. Hnatejko, M. Kubicki, J. Kłak, M. J. Korabik and V. Patroniak, *Polyhedron*, 2011, **30**, 730–737.

59 F. Ni, Z. Zhu, X. Tong, M. Xie, Q. Zhao, C. Zhong, Y. Zou and C. Yang, *Chem. Sci.*, 2018, **9**, 6150–6155.

60 Y. Ding, F. Wang, Z. Ku, L. Wang and H. Zhou, *J. Struct. Chem.*, 2009, **50**, 1212–1215.

61 J. Li, R. Liu, J. Jiang, X. Liang, L. Huang, G. Huang, H. Chen, L. Pan and Z. Ma, *Molecules*, 2019, **24**, 4519.

62 N. Busto, P. Calvo, J. Santolaya, J. M. Leal, A. Guédin, G. Barone, T. Torroba, J.-L. Mergny and B. García, *Chem. - A Eur. J.*, 2018, **24**, 11292 – 11296.

63 L. Hahn, N. J. Buurma and L. H. Gade, *Chem. - A Eur. J.*, 2016, **22**, 6314–6322.

64 A. Funke, J. Dickerhoff and K. Weisz, *Chem. - A Eur. J.*, 2016, **22**, 3170–3181.

65 A. Łęczkowska, J. Gonzalez-Garcia, C. Perez-Arnaiz, B. Garcia, A. J. P. White and R. Vilar, *Chem. - A Eur. J.*, 2018, **24**, 11785–11794.

66 D. Drygin, A. Siddiqui-Jain, S. O'Brien, M. Schwaebe, A. Lin, J. Bliesath, C. B. Ho, C. Proffitt, K. Trent, J. P. Whitten, J. K. C. Lim, D. Von Hoff, K. Anderes and W. G. Rice, *Cancer Res.*, 2009, **69**, 7653–7661.

View Article Online
DOI: 10.1039/D0DT02125C

TOC Graphic Material

SYNOPSIS TOC: The synthesis and SAR study of a family of Zn(II) terpyridine derivatives with leaving groups (X: Cl or NO_3) and different 4´substituents (R) was performed. The leaving group and the R play a role in cytotoxicity whereas only the latter governs the thermal stabilization of G-quadruplex structures. The fluorescent complex **3Cl** (X=Cl, L3), which is localized in the nucleus, is the most cytotoxic derivative and displays high affinity towards the human telomeric G-quadruplex Tel22.